Vietnam Journal of Science and Technology
DOI: https://doi.org/10.15625/2525-2518/20799

Novel distributed control for multi-agent systems: Application to a quadcopter formation

M. Xuan Nguyen*

Faculty of Engineering, Dong Nai Technology University, Dong Nai Province, Viet Nam

*Email: *nguyen_xuan@dntu.edu.vn*

Received: 15 May 2024; Accepted for publication: 15 October 2024

Abstract. Multi-agent systems (MAS) are well-known for overweighting single agents that exhibit several complex tasks. This paper introduces a novel approach to modeling and controlling an MAS employing a directed and switchable topology. The interaction dynamics of the MAS are described through a mass–spring system, where individual agents are modeled as point masses and their relative positions are represented by virtual elastic links that produce coordination forces. A notion of formation equilibrium is introduced to describe the steady-state configuration of the network, which is characterized via the underlying interaction forces. By examining these equilibrium conditions, a distributed control strategy is constructed to guarantee convergence toward the prescribed geometric configuration. The performance and validity of the proposed method are verified through comprehensive simulation studies.

Keywords: distributed control, multi-agent system, formation control, quadcopter.

Classification numbers: 5.3.7, 5.8, 5.10.2.

1. INTRODUCTION

Over the past decade, consensus control of multi-agent systems has gained substantial research interest, particularly in the context of quadrotor formation missions [1-4]. Compared with other categories of unmanned aerial platforms, quadrotors provide notable advantages, including agile motion capability, relatively simple mechanical architecture, dependable operation, and economic feasibility. Consequently, they have been widely deployed across various practical domains such as environmental assessment, atmospheric observation, emergency response, reconnaissance, infrastructure inspection, and aerial surveying. Operating multiple quadrotors cooperatively offers clear performance enhancements over single-vehicle missions, including higher collective payload capacity, distributed sensing functionality, extended coverage range, and improved capability in executing sophisticated tasks [5]. However, achieving consensus formation behavior introduces significant technical challenges, as it involves rigorous treatment of system modeling, distributed control synthesis, and inter-agent communication mechanisms.

A broad spectrum of formation control strategies has been reported for cooperative quadrotor systems. Early contributions, such as [6, 7], primarily relied on leader-follower architectures. Nevertheless, these approaches were typically confined to planar (two-dimensional) formation scenarios and did not explicitly incorporate inter-agent relative

displacement constraints for three-dimensional shape preservation. Alternative studies, for example [8], focused on flock formation control but solely addressed shape-keeping without mentioning formation pattern-achieving. Other works [9-14] formulated formation control under consensus-based frameworks employing either undirected communication graphs or static interaction topologies. Although mathematically elegant, such methods often impose substantial communication overhead and exhibit limited scalability in large-scale deployments.

To overcome these shortcomings, more recent investigations have explored formation coordination under directed and time-varying interaction graphs. In [15], a consensus-oriented strategy was developed for UAV networks with directed switching topologies. Similarly, [16] introduced a formation algorithm for second-order multi-agent systems. Despite these efforts, challenges persist, with limited research capable of providing a formation control algorithm accommodating both directed and switching topologies. The references above underscore the ongoing challenge faced by worldwide researchers in achieving formation control for multiple UAVs. Indeed, most existing methods are restricted to either undirected graphs or fixed topological configurations, with only a limited number accommodating the coexistence of directed and switching interactions.

Motivated by these observations, this study investigates the formation structure and associated control law for cooperative quadrotor systems. A novel modeling and control framework is developed based on a mass-spring-inspired interaction mechanism, where inter-agent couplings are represented through virtual elastic forces. Each quadrotor is modeled as a rigid body interconnected with neighboring agents via formation springs, leading to a compact linear state-space representation of the overall formation dynamics. On this basis, an equilibrium-based formation controller is designed using an integral linear quadratic regulator (LQR) formulation to ensure optimal regulation of the formation error dynamics. The overall architecture adopts a hierarchical structure comprising distributed high-level and low-level controllers. Specifically, a distributed algorithm at the high level generates reference trajectories for each agent, while low-level PID-based tracking controllers ensure accurate position regulation.

Compared with existing approaches, the proposed framework offers several distinctive advantages. First, the mass-spring modeling paradigm provides an intuitive yet rigorous representation of formation dynamics, facilitating systematic stability and controllability analysis. Second, the proposed distributed control laws explicitly accommodate directed and switching communication topologies. Third, the resulting scheme is computationally efficient, making it suitable for real-time implementation in resource-constrained UAV platforms. Finally, extensive numerical simulations are conducted to validate the effectiveness and robustness of the proposed methodology.

2. PRELIMINARIES AND PROBLEM STATEMENT

2.1. Two-mass – one-spring system

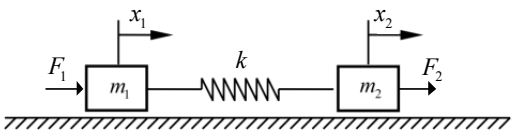

Figure 1. A two-mass – one-spring system consists of two masses connecting via a spring.

Consider a viscous friction-free mechanical system, as in Figure 1. The system consists of two masses, namely m_1 and m_2, connecting to each other via a spring k.

Let vector $x=[x_1,x_2]^T \in \sim^2$ represents the displacement of m_1, m_2 from a predefined origin, and vector $F=[F_1, F_2]^T \in \sim^2$ denotes external forces applied to each mass (see Figure 1). Thus, we have:

$$\begin{bmatrix} m_1 & 0 \\ 0 & m_2 \end{bmatrix}\begin{bmatrix} \ddot{x}_1 \\ \ddot{x}_2 \end{bmatrix}+\begin{bmatrix} k & -k \\ -k & k \end{bmatrix}\begin{bmatrix} x_1 \\ x_2 \end{bmatrix}=\begin{bmatrix} F_1 \\ F_2 \end{bmatrix} \tag{1}$$

Manipulating (1), one can get:

$$\ddot{x}_2-\ddot{x}_1+\frac{k(m_1+m_2)}{m_1m_2}(x_2-x_1)=\frac{F_2}{m_2}-\frac{F_1}{m_1} \tag{2}$$

Let us define the following state variable, representing the relative position and velocity between the masses.

$$\varepsilon=\begin{bmatrix} x_2-x_1 \\ \dot{x}_2-\dot{x}_1 \end{bmatrix} \tag{3}$$

Then, Eq. (2) can be reformulated as:

$$\begin{cases} \dot{\varepsilon}=A\varepsilon+Bu \\ \zeta=C\varepsilon \end{cases} \tag{4}$$

where,

$$A=\begin{bmatrix} 0 & 1 \\ -\dfrac{k(m_1+m_2)}{m_1m_2} & 0 \end{bmatrix}, B=\begin{bmatrix} 0 \\ 1 \end{bmatrix}, C=\begin{bmatrix} 1 & 0 \\ 0 & 1 \end{bmatrix}, u=\frac{F_2}{m_2}-\frac{F_1}{m_1} \tag{5}$$

2.2 Quadcopter dynamics

Let $\phi, \theta,$ and ψ respectively represent the roll, pitch, and yaw angles ($|\phi|<\pi/2$ and $|\theta|<\pi/2$) of the quadcopter; x, y, and z position in the inertial coordinate system (Figure 2). Let $I=\text{diag}[I_1, I_2, I_3]$ be the inertia momentums in the body-fixed coordinate system, m the mass, and l_a the arm length of vehicle; $u=[u_T, u_p, u_q, u_r]^T$ is the control input, and g is the gravitational acceleration. Then, the quadcopter dynamics can be described as follows [17]:

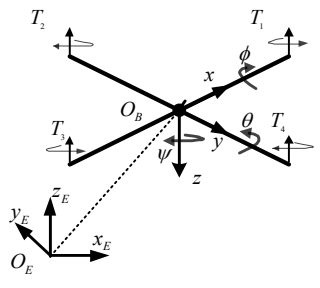

Figure 2. The quadcopter consists of four motors, out of which two motors (1 and 3) rotate counterclockwise, and the other two (2 and 4) rotate clockwise.

$$\begin{cases} \dot{p} = \left(\dfrac{I_2 - I_3}{I_1}\right) qr + \dfrac{1}{I_1} u_p \\ \dot{q} = \left(\dfrac{I_3 - I_1}{I_2}\right) rp + \dfrac{1}{I_2} u_q \\ \dot{r} = \left(\dfrac{I_1 - I_2}{I_3}\right) pq + \dfrac{1}{I_3} u_r \\ \ddot{x} = \dfrac{1}{m}\left(\cos\phi \sin\theta \cos\psi + \sin\phi \sin\psi\right) u_T \\ \ddot{y} = \dfrac{1}{m}\left(\cos\phi \sin\theta \sin\psi - \sin\phi \cos\psi\right) u_T \\ \ddot{z} = g - \dfrac{1}{m}\left(\cos\phi \cos\theta\right) u_T \end{cases} \tag{6}$$

The control input u is computed from the motor's forces, $T_i = c_T \Omega_i^2, (i = 1,2,3,4)$, as follows

$$\begin{cases} u_T = T_1 + T_2 + T_3 + T_4 \\ u_p = l_a (T_2 - T_4) \\ u_q = l_a (T_1 - T_3) \\ u_r = c_D \left(T_1 + T_3 - T_2 - T_4\right) \end{cases} \tag{7}$$

where, Ω_i is the i th-motor's speed; c_T and c_D stand for the thrust and drag coefficients.

2.3. Preliminaries

Assumption 1 *(inter-agent communication topology):* The communication graph is assumed to be complete and symmetric, implying that every quadrotor can exchange state information with all other vehicles.

Notation 1: Consider a cooperative quadrotor system consisting of *n* agents. Define the index set as $D = \{1, 2, \ldots, n\}$. M_i represents *i*th quadcopter ($i \in D$). Without loss of generality, M_1 is designated as the leader. Let F_{ij} denote the virtual spring force exerted on agent M_i by M_j. This interaction satisfies the anti-symmetry condition is denoted by $F_{ij} = -F_{ji}$ and $F_{ii} = 0$. The resultant formation force acting on agent M_i is given by $F^{(i)} = \sum_{j=1}^{N} F_{ij}$. Vector $\rho_i = \left(x_i, y_i, z_i\right)$ and $\Theta_i = \left(\phi_i, \theta_i, \psi_i\right)$ respectively represent the translational position and attitude of M_i.

2.4. Control objective

The control scheme of each agent involves two loops, i.e., high-level and low-level controllers. While the high-level loop plays the role of generating referenced trajectory ρ_d, the

low-level loop guarantees that the vehicle tracks the references. The integration of the two loops is to force the formation error to zero, i.e., $\lim_{t\to\infty}(\rho-\rho_d)=0$. The main results of this work focus on finding a novel high-level control law, which will be called formation controller hereafter.

3. MAIN RESULTS

3.1. Mass-spring system-based MAS's dynamics model

In order to utilize the mass-spring system concept for the dynamic modelling of a MAS, the following definitions are introduced.

Definition 1 *(formation spring):* A formation spring refers to a virtual coupling established between the spatial positions of any two agents within the formation. Each terminal of the spring is anchored to one agent (see Fig. 3). The stiffness coefficient of the formation spring is denoted by K_f, which characterizes the strength of the inter-agent interaction. The stiffness parameter is expressed in units of N/m.

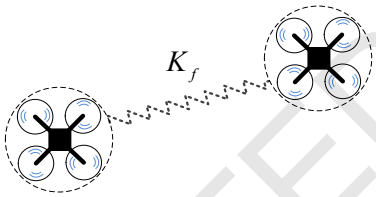

Figure 3. Illustration of a formation spring modeling the interaction between the positions of two agents.

Definition 2 *(formation force):* The force generated by a formation spring is referred to as the formation force and is denoted by F_f. This force satisfies the following characteristics:

- The direction of F_f is colinear with the direction of the formation spring.

- The magnitude of F_f varies proportionally with the spring deformation (elongation or compression), denoted by Δl.

$$F_f=-K_f\Delta l \tag{8}$$

Definition 3 *(formation equilibrium state of an agent):* An agent is said to be in a formation equilibrium state when the resultant of all formation forces acting upon it becomes zero. That is,

$$\sum F_f=0 \tag{9}$$

Definition 2 indicates that the formation forces are independent of the mass of the agents. Thus, for the sake of simplicity, all mass of the agents are set as *m,* and all formation spring's stiffness are set as K_f.

$$\begin{bmatrix} m & 0 & \cdots & 0 \\ 0 & m & \cdots & 0 \\ \vdots & \vdots & \ddots & \vdots \\ 0 & 0 & \cdots & m \end{bmatrix}\begin{bmatrix} \ddot{\rho}_1 \\ \ddot{\rho}_2 \\ \vdots \\ \ddot{\rho}_n \end{bmatrix}+\begin{bmatrix} (n-1)K_f & -K_f & \cdots & -K_f \\ -K_f & (n-1)K_f & \cdots & -K_f \\ \vdots & \vdots & \ddots & \vdots \\ -K_f & -K_f & \cdots & (n-1)K_f \end{bmatrix}\begin{bmatrix} \rho_1 \\ \rho_2 \\ \vdots \\ \rho_n \end{bmatrix}=\begin{bmatrix} F_1 \\ F_2 \\ \vdots \\ F_n \end{bmatrix} \tag{10}$$

In (10), subtracting the *i*-th row by the first-row yields:

$$m(\ddot{\rho}_i - \ddot{\rho}_1) + n_i K_f(\rho_i - \rho_1) = F_i - F_1 \tag{11}$$

Let

$$\varepsilon_i = \begin{bmatrix} \rho_i - \rho_1 \\ \dot{\rho}_i - \dot{\rho}_1 \end{bmatrix} \tag{12}$$

Then

$$\begin{cases} \dot{\varepsilon}_i = A_i \varepsilon_i + B_i u_i \\ \zeta_{i1} = C_i \varepsilon_i \end{cases} \tag{13}$$

where,

$$A_i = \begin{bmatrix} 0 & 1 \\ -\dfrac{n_i K_f}{m} & 0 \end{bmatrix}, B_i = \begin{bmatrix} 0 \\ 1 \end{bmatrix}, C_i = \begin{bmatrix} 1 & 0 \\ 0 & 1 \end{bmatrix}, u_i = \frac{1}{m}(F_i - F_1) \tag{14}$$

3.2. Formation controller

The formation controller, presented in this subsection, consists of two parts, i.e., the reference generator and the formation equilibrium state controller.

3.2.1. Reference generator

We next develop the reference generation mechanism for the formation. The interaction force exerted on agent M_i due to its coupling with agent M_j is modeled as

$$F_{ji} = -K_f(x_i - x_j) \tag{15}$$

Under Assumption 1 (complete bidirectional connectivity), the cumulative formation force acting on agent M_i can be expressed as

$$\sum F^{(i)} = F_i - K_f \sum_{j=1}^{n} (x_i - x_j) \tag{16}$$

For proper formation maintenance, the resultant formation force on each quadrotor is required to be zero during flight. Therefore, the equilibrium condition is formulated as

$$\sum F^{(1)} = F_1 - K_f \sum_{j=2}^{n} (x_1 - x_j) = 0 \tag{17}$$

or

$$F_1 = K_f \sum_{j=2}^{n} (x_1 - x_j) \tag{18}$$

From (14), we have:

$$F_i = mu_i + F_1 \tag{19}$$

From (16), (18), and (19), the following are obtained:

$$\begin{aligned} \sum F^{(i)} &= mu_i + K_f \sum_{j=2}^{n} (x_1 - x_j) - K_f \sum_{l=1}^{n} (x_i - x_l) \\ &= mu_i - K_f \left[\sum_{j=2}^{n} x_j - (n-1)x_1 \right] - K_f \left[nx_i - x_1 - \sum_{l=2}^{n} x_l \right] \\ &= mu_i - nK_f (x_i - x_1) \end{aligned} \tag{20}$$

This total force $\sum F^{(i)}$ drives M_i toward the position x_i^d which satisfies:

$$\sum F^{(i)} = K_f \sum_{j=1}^{n} (x_i^d - x_j) \tag{21}$$

which can be rewritten as:

$$mu_i - nK_f (x_i - x_1) = K_f \sum_{\substack{j=1 \\ j \neq i}}^{n} (x_i^d - x_j) = K_f \left[(n-1)x_i^d - x_1 - \sum_{\substack{j=2 \\ j \neq i}}^{n} x_j \right] \tag{22}$$

Manipulating (22), we obtain:

$$x_i^d = \frac{m}{(n-1)K_f} u_i - \frac{1}{n-1} \left[nx_i - \sum_{\substack{j=2 \\ j \neq i}}^{n} x_j - (n+1)x_1 \right] \tag{23}$$

Remark 3: The proposed scheme operates in a distributed manner, where the control law is locally executed on each quadrotor. The reference trajectory for every agent is generated using its own state feedback together with relative state information obtained from neighboring agents.

3.2.2. Formation equilibrium state controller (FESC)

To examine the controllability of system (13), the controllability matrix C_m is constructed as:

$$C_m = [B_i \quad A_i B_i] = \begin{bmatrix} 0 & 1 \\ 1 & 0 \end{bmatrix} \tag{24}$$

It can be readily verified that has full rank. Hence, system (13) satisfies the controllability condition.

The overall control architecture of each quadrotor is organized in a hierarchical two-layer structure, consisting of a high-level controller and a low-level controller, as illustrated in Figure 4.

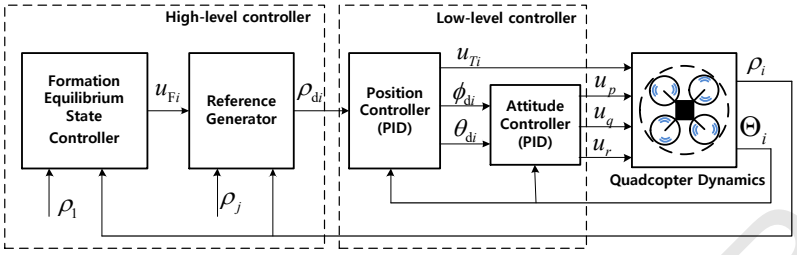

Figure 4. The distributed control scheme is implemented on each agent in the high-level controller.

The FESC is formulated based on an integral linear quadratic regulator (LQR) framework. The corresponding control input is expressed as

$$u_{Fi} = -\gamma \xi_i + \gamma_I \int_0^t e_\zeta \, \mathrm{d}\tau \tag{25}$$

where, $e_\zeta = \zeta_{i1d} - \zeta_{i1}$. γ and γ_I are positive gains to be chosen.

The control laws in (25) can be described by a block diagram, as shown in Figure 5.

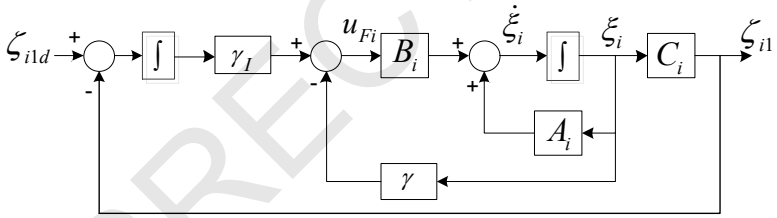

Figure 5. Block diagram of the proposed FESC.

Remark 1: It is obvious that ζ_{ij} converges to $\zeta_{ij\mathrm{d}}$ because ζ_{i1} and ζ_{j1} simultaneously converge to $\zeta_{i1\mathrm{d}}$ and $\zeta_{j1\mathrm{d}}$, respectively.

Remark 2: The inclusion of the integral action in (25) guarantees zero steady-state error under constant disturbances or model uncertainties.

4. SIMULATION RESULTS AND DISCUSSIONS

4.1. Simulation Setup

The numerical experiments are carried out under the following assumptions: (i) the attitude of each quadrotor is obtained from an inertial navigation system (INS); (ii) altitude measurements are provided by a ranging sensor; and (iii) horizontal position data are acquired

via a GPS module. The dynamic parameters adopted for the quadrotor model are summarized in Table 1.

To validate the effectiveness of the proposed control strategy, formation flight simulations are performed under two distinct communication topologies, denoted as Topology 1 and Topology 2, as illustrated in Figure 6. Each green arrow in Figure 6 indicates a directed information exchange link between a pair of agents. For instance, in Topo. 1, agent M_2 directly accesses information from the virtual leader M_1, while M_3 only has access to information from M_2, and so forth. Meanwhile, Topo. 2 is configured in a reverse manner, presenting an alternative arrangement of inter-communication dynamics.

The leader's trajectory is predefined as: $(x^d, y^d, z^d) = (0.3t, 0.3t, 0.3t)$. The desired formation geometry is specified through prescribed relative displacement vectors between agents: $\zeta_{21}^d = [0,1,0]^T$, $\zeta_{32}^d = [-1,-2,0]^T$, $\zeta_{43}^d = [2,0,0]^T$, and $\zeta_{14}^d = [-1,1,0]^T$. The initial states, including position and velocity, of the quadcopters are provided in Table 2.

Table 1. Quadcopter dynamic parameters used in the simulations.

Symbol	Value and unit
m	1.80 kg
I_1	0.0121 kg.m^2
I_2	0.0119 kg.m^2
I_3	0.0223 kg.m^2
l_a	0.23 m
g	9.81 m/s^2

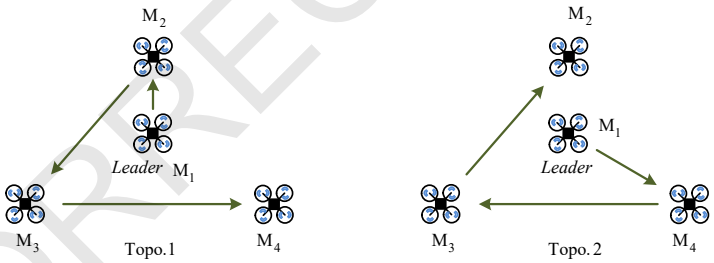

Figure 6. Two inter-communication topologies (Topo. 1 and Topo. 2) are used in the simulation. The agents are desired to form a triangle formation pattern with the leader at the center and the others at the corners.

Table 2. Initial positions of the quadcopters

Symbol	Value and unit
$p_1(0)$	$[0,0,0]^T$
$p_2(0)$	$[-0.5,1.5,0]^T$
$p_3(0)$	$[-1.5,-1.5,0]^T$
$p_4(0)$	$[1.5,-1.2,0]^T$

4.2. Simulation results

In Stage 1, the simulation is conducted over the interval $t \in [0,50]$ s. At the initial time, all quadrotors are initialized at their prescribed starting positions and subsequently begin motion. Under the action of the proposed controller, the agents track the reference trajectory and reach convergence within a few seconds, as illustrated in Figures 7 and 8. The settling time is approximately 7 s for all vehicles. Due to the specified communication topology, transient oscillatory behavior is observed in the position responses, as shown in Fig. 8(a). For agent M_2, the oscillations are 0.1 m, 0.12 m, and 0.11 m along the x-, y-, and z-axis, respectively. Quadcopter M_3 exhibits oscillations of 0.15 m, 0.08 m, and 0.21 m in the corresponding directions. Similarly, the position responses of M_4 experiences oscillations of 0.3 m, 0.06 m, and 0.27 m for its x-, y-, and z-positions. The velocity profiles converge to their steady-state values after a brief transient phase, as presented in Fig. 8(b). The rapid stabilization of both position and velocity responses enables the formation to be established efficiently while maintaining accurate tracking of the desired trajectory.

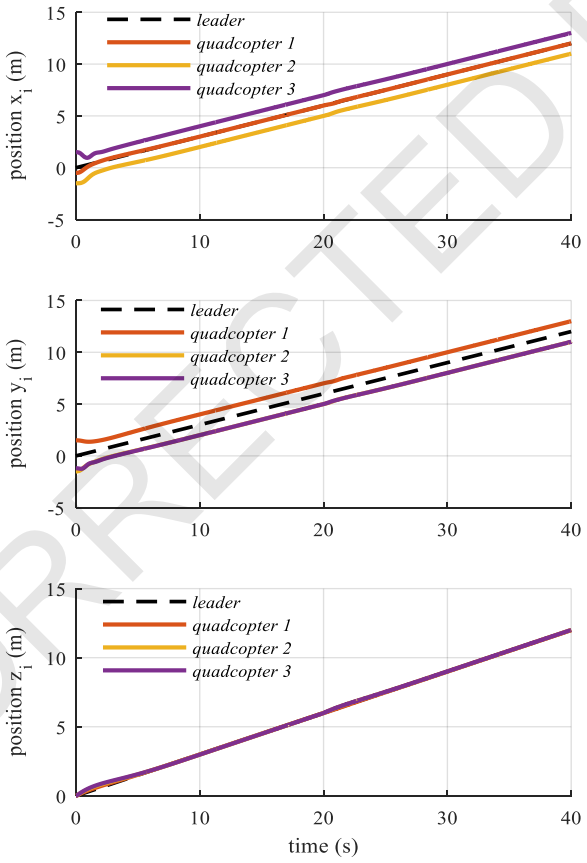

Figure 7. Formation convergence and three-axis trajectory tracking performance of the multi-agent system.

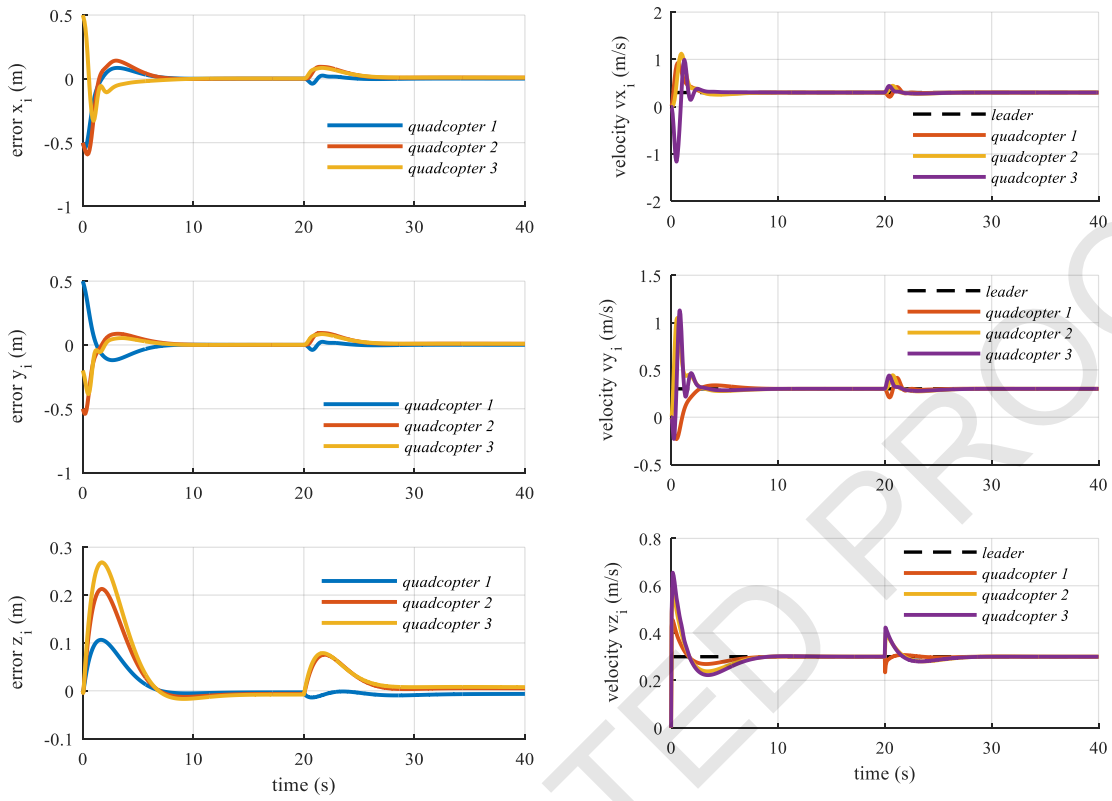

Figure 8. Position (a) and velocity (b) tracking error performance of the multi-agent system.

At $t = 20$ s, the second simulation phase (Stage 2) is initiated by switching the communication topology from Topology 1 to Topology 2. This abrupt topology transition induces transient oscillatory responses in the formation dynamics. As shown in Fig. 8, the peak-to-peak oscillation amplitudes in position tracking remain below 0.1 m along the x-, y-, and z-positions. Despite the temporary fluctuations, the formation geometry is quickly restored, and stable trajectory tracking is re-established within approximately 6 s. In practical deployment scenarios, such topology variations may arise from operator intervention or unexpected system faults. The fast transient response exhibited by the proposed control strategy suggests strong potential for reliable and efficient formation flight operations under switching communication structures, particularly in missions involving complex collective tasks.

5. CONCLUSIONS

This paper presents a distributed control framework for multi-agent systems based on a mass–spring interaction model. The derived formation dynamics are utilized to synthesize the formation controller, which is applied to a quadrotor formation flight problem under time-varying communication topologies. Simulation results confirm that the proposed approach achieves accurate formation acquisition, precise trajectory tracking, and robust maintenance of the formation shape during topology transitions. It should be noted that the formation interaction was modeled using an idealized mass–spring representation, without explicitly

accounting for communication delays, packet losses, or external disturbances. Future research will focus on the development of robust or adaptive formation control strategies capable of compensating for uncertainties and perturbations in practical multi-UAV deployments.

CRediT authorship contribution statement. M. Xuan Nguyen: Methodology, Investigation, Funding acquisition, Simulation, Writing, Supervision.

Declaration of competing interest. The authors declare that they have no known competing financial interests or personal relationships that could have appeared to influence the work reported in this paper.

REFERENCES

1. Idrissi M., Salami M., Annaz F. - A Review of Quadrotor Unmanned Aerial Vehicles: Applications, Architectural Design and Control Algorithms. Journal of Intelligent & Robotic Systems, **104**(2) (2022) 1-33. https://doi.org/10.1007/s10846-021-01527-7.
2. Lee J.-W., Xuan-Mung N., Nguyen N. P., Hong S. K. - Adaptive altitude flight control of quadcopter under ground effect and time-varying load: theory and experiments. Journal of Vibration and Control, **29**(3–4) (2023) 571-581. https://doi.org/10.1177/10775463211050169.
3. Chamola V., Kotesh P., Agarwal A., Naren, Gupta N., Guizani M. - A Comprehensive Review of Unmanned Aerial Vehicle Attacks and Neutralization Techniques. Ad Hoc Networks, **111** (2021) 102324. https://doi.org/10.1016/j.adhoc.2020.102324.
4. Do T.-D., Xuan-Mung N., Lee Y.-S., Hong S. K. - 2023 9th International Conference on Control, Decision and Information Technologies (CoDIT), IEEE, (2023) 2151-2157. https://doi.org/10.1109/codit58514.2023.10284286.
5. Abbas R., Wu Q. - Tracking Formation Control for Multiple Quadrotors Based on Fuzzy Logic Controller and Least Square Oriented by Genetic Algorithm. The Open Automation and Control Systems Journal, **7**(1) (2015) 842-850. https://doi.org/10.2174/1874444301507010842.
6. Abbas R., Wu Q. - Improved Leader Follower Formation controller for multiple Quadrotors based AFSA. TELKOMNIKA (Telecommunication Computing Electronics and Control), **13**(1) (2015) 85-92. https://doi.org/10.12928/telkomnika.v13i1.994.
7. Abas M. F. B., Ali S. A. M., Iwakura D., Song Y., Nonami K. - MAV Circular Leader-Follower Formation Control Utilizing Mass-Spring-Damper with Centripetal Force Consideration. Journal of Robotics and Mechatronics, **25**(1) (2013) 240-251. https://doi.org/10.20965/jrm.2013.p0240.
8. Xue R., Song J., Cai G. - Distributed formation flight control of multi-UAV system with nonuniform time-delays and jointly connected topologies. Proceedings of the Institution of Mechanical Engineers, Part G: Journal of Aerospace Engineering, **230**(10) (2016) 1871-1881. https://doi.org/10.1177/0954410015619446.
9. Dong X., Yu B., Shi Z., Zhong Y. - Time-Varying Formation Control for Unmanned Aerial Vehicles: Theories and Applications. IEEE Transactions on Control Systems Technology, **23**(1) (2015) 340-348. https://doi.org/10.1109/tcst.2014.2314460.
10. Dong X., Zhou Y., Ren Z., Zhong Y. - Time-varying formation control for unmanned aerial vehicles with switching interaction topologies. Control Engineering Practice, **46** (2016) 26-36. https://doi.org/10.1016/j.conengprac.2015.10.001.

11. Abbas R., Wu Q. - Adaptive Leader Follower Control for Multiple Quadcopters via Multiple Surfaces Control. Journal of Beijing Institute of Technology, **25**(4) (2016) 526-532. https://doi.org/10.15918/j.jbit1004-0579.201625.0411.

12. Du H., Zhu W., Wen G., Duan Z., Lu J. - Distributed Formation Control of Multiple Quadrotor Aircraft Based on Nonsmooth Consensus Algorithms. IEEE Transactions on Cybernetics, **49**(1) (2019) 342-353. https://doi.org/10.1109/tcyb.2017.2777463.

13. Zhou Z., Wang H., Hu Z. - Event-Based Time Varying Formation Control for Multiple Quadrotor UAVs with Markovian Switching Topologies. Complexity, **2018**(1) (2018) 8124861. https://doi.org/10.1155/2018/8124861.

14. Qi Y., Zhou S., Kang Y., Yan S. - Formation Control for Unmanned Aerial Vehicles with Directed and Switching Topologies. International Journal of Aerospace Engineering, **2016** (2016) 1-8. https://doi.org/10.1155/2016/7657452.

15. Li Y., Dong X., Li Q., Ren Z. - 2017 36th Chinese Control Conference (CCC), IEEE, (2017) 8530-8535. https://doi.org/10.23919/chicc.2017.8028710.

16. Xuan-Mung N., Hong S.-K. - Improved Altitude Control Algorithm for Quadcopter Unmanned Aerial Vehicles. Applied Sciences, **9**(10) (2019) 2122. https://doi.org/10.3390/app9102122.

17. Ganji S. S., Barari A., Ganji D. D. - Approximate analysis of two-mass-spring systems and buckling of a column. Computers and Mathematics with Applications, **61**(4) (2011) 1088-1095. https://doi.org/10.1016/j.camwa.2010.12.059.